INFLUENCE OF THE MICROSTRUCRURE ON CAVITATION EROSION RESISTANCE OF CAST IRON WITH NODULAR GRAPHITE

PhD thesis – Summary
To obtain the scientific title of doctor at
Polytechnic University of Timișoara
in the field of Material engineering

author ing. Aurel Traian BENA

Scientific leaders: Prof. univ .dr. ing. Ion MITELEA and Prof. univ. dr.ing. Ilare Bordeaşu
month__ year 2019

Chapters 1

CURRENT STATE OF RESEARCH ON CAVITATION EROSION OF CAST-IRON WITH NODULAR GRAPHITE

1.3 Cavitational erosion: factors of influence, degradation mechanisms

Cavitational erosion is considered by specialists as a typical phenomenon of local fatigue of the material that suffers deformations and / or breaks under repeated impact with microjet and shock waves generated by cavitation bubble implants [35], 72], [61].
Cavitation erosion degradation occurs in various equipment such as pumps, hydraulic turbines, naval propellers, rotors and high speed mixers in the pharmaceutical, aerospace, chemistry and petrochemistry industries but also other hydromechanical equipment [72], [5] [6].
At present, both scientists and manufacturers of hydromechanics, marine and river vessels are concerned about finding new materials and new techniques to improve cavitation erosion.
Research conducted in specialized laboratories [34], [5], [66], [6] showed that the level of cavitational damage to steels depends, on the one hand, on the intensity of the cavitation, which is specific to the hydrodynamics of the cavitational current, and on another part, of the nature of the material characterized by:

- chemical composition, namely carbon content and alloying elements (Ni, Cr, Mn, Mo, V, W, Nb, Al); - microstructure;
- technology for the production of the semi
- finished product (cast, laminate, etc.);
- treatment and structural homogenization (thermal, thermomechanical, thermochemical, etc.);
- the value of the mechanical properties (Rm, Rp0,2, HB, KCU

During cavitation, in the hydrodynamic current, through the variation of pressures, the cavitational bubbles develop which may be symmetrical or asymmetrical according to where they are. The asymmetrical shape occurs when the bubble is close to the solid wall. The closer it is to the solid, the more it deforms. Due to the pressure increase, two phenomena occur: the bubble compresses to a point - a phenomenon called implosion - and when it passes through a smaller pressure field it suddenly relaxes and generates shock waves whose impact on the solid is 104- 106 atm. [79], [56]. The impact force decreases when the bubble is further away from the wall and the fluid is more viscous. The duration of the transition from the small size to the sudden expansion is in the order of the microseconds, and therefore the shock wave impacting the solid has a very high force.

The second mechanism is that of microjet jets. These microjet jets appear in an annular whirlpool due to the involution of the bubble wall much more pronounced when it is near the wall. The bulk wall of the bubble is pushed outward until the bubble breaks and a microjet with a diameter of less than 1 mm and at a speed of up to 100 m / s is created [79], [21]. The mechanism of involution of the bubble wall and the appearance of microjet is presented in **Figures 1.7** and **1.8** [10], [11]. In **Figure 1.8**, it is also suggested how the material breaks (crack propagation) after impact with the microjet.

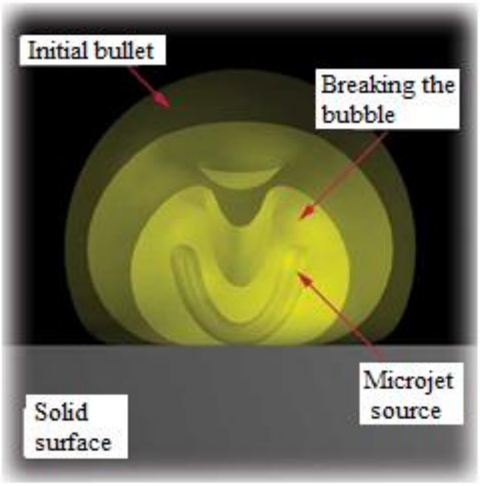

Fig. 1.7 The cavitation bubble and microjet molding mechanism [10], [11]

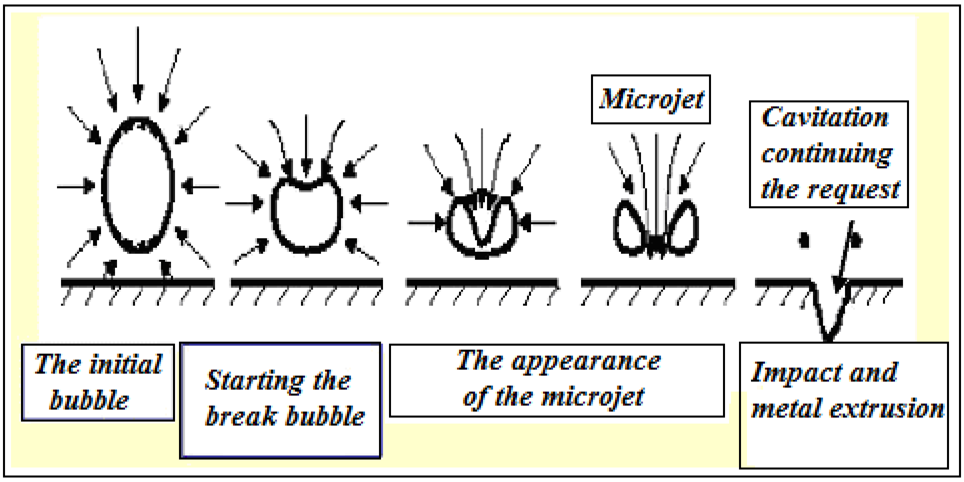

Fig. 1.8 The mechanism of cavitation bubble and crack generation [10], [11]

1.6 The difficulty of the problem

Standardized tests that simulate the cavitation erosion process under laboratory conditions lead to significant differences from the actual cavitation phenomena occurring in hydraulic machine components. Thus, Choi et al. [27] studied the influence of different erosion intensities and test methods and concluded that the relative classification of the erosion resistance of some materials depends on the intensity of the cavitation. According to Chahine et al. [26], the ultrasound test method leads to the formation of a cloud of cavitation bubbles, always in the same place, with nearly uniform bubbles and a form of them obtained at a fixed frequency, compared to real cases where there is a distribution of magnitude as well as different interesting frequencies. They also emphasized that the standardized test does not allow a full characterization of behavior under real conditions due to the absence of a real fluid flow or the interaction of bubble nuclei with turbulent flow vortices.

Compared to the actual cavitation erosion that occurs after a long exposure period, standardized accelerated tests provide relevant laboratory results that can be used to compare tested materials under similar conditions. The equipment used for this purpose leads to an intense erosion process in a controllable and reproducible manner, by generating bubble clouds that erode the surface of a sample made from the test material. Such equipment can be used to evaluate the cavitation erosion resistance of a material in terms of erosion speed, thus allowing a classification of the materials based on this property. Ultrasonic equipment has been developed to evaluate the cavitation erosion process, according to ASTM standards G32-2010 [9], 29]. They have the advantage of using simple equipment with easily controllable parameters, generating longitudinal vibrations, amplified and transmitted in the fluid like ultrasonic waves.

Another difficulty of the problem under consideration is the multiple unsuccessful or only partially successful attempts to correlate cavitation erosion resistance with one or a combination of mechanical properties of metallic materials. These mechanical properties include the characteristics of ductility, hardness, tear strength, flow limit, KCU resilience, KV breaking energy [17] and the product of fatigue strength coefficient and cyclic mechanical eccentric exponent [34]

Franc and Michel [35] pointed out that fatigue mechanisms should be expected due to the repetitive nature of the process, involving high demand rates and short impact times.

1.7 Objectives of the PhD thesis

The research carried out within the doctoral thesis aims at the following main objectives:

- the effect of volumetric thermal treatments on cavitation erosion resistance;
- generating submicro- and nano-structured layers with increased resistance to cavitation erosion using modern surface modification techniques;
- Deepening the mechanism of priming and propagation of cracks and tears following the stresses caused by the impact of microjet and shock waves on the implosion of cavitation bubbles in the hydrodynamic field.

The aim of the research is to find comprehensive interdisciplinary solutions and to establish the potential of measures focusing on thermal treatments and coatings of metallic surfaces with new materials with improved anticatrial performance.

The novelty of the PhD thesis:

The novelty of the PhD thesis consists in the phenomenological deepening of the cavitation erosion and the definition of the ways of enriching the surface of the nodular casting in order to increase the life of the equipment working in such conditions.

Chapters 2

VOLUMETRIC THERMAL TREATMENTS AND RESISTANCE TO CAVITATION EROSION

2.2 Investigated material, experimental stand and working procedure

The investigated material is a ferrite-perlite matrix, EN-GJS-400-15, having the following chemical composition: C = 3.57%, Si = 2.51%, Mn = 0.23%, P = 0.044%, S = 0.010% Fe = rest.
In the unattached state, the graphite form is completely spherical, with about 50-70 nodules / m2, whose average size varies between 40 μm and 60 μm (**Figure 2.1a).** The base metal microstructure consists of approximately 60% F and 40% P (**Figure 2.1b).**

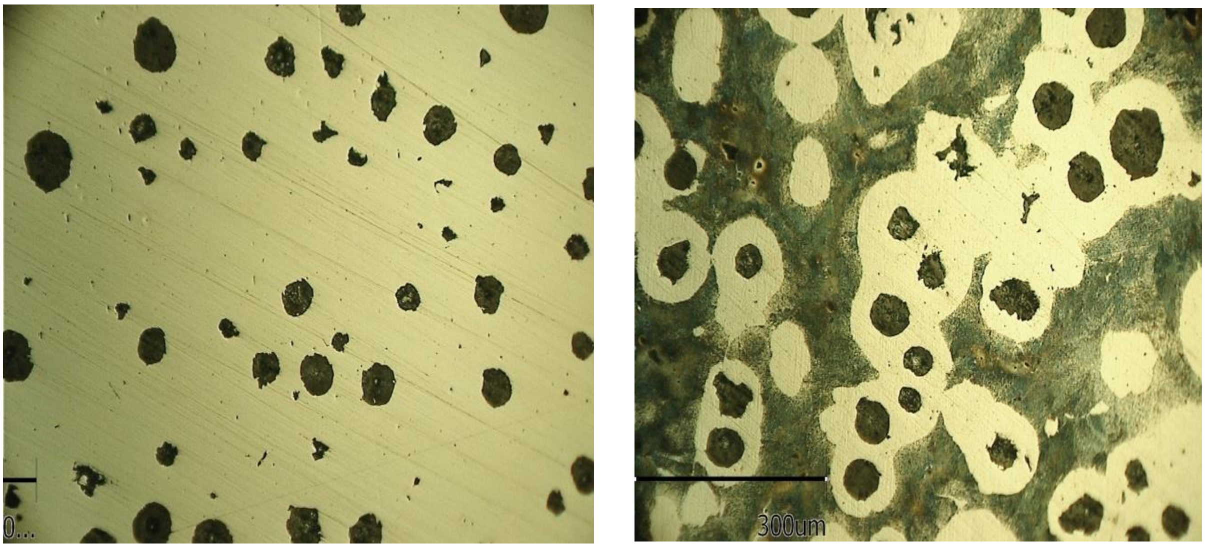

-a- x 100 **-b- x100**

Fig. 2.1 Graphite morphology **(a)** and microstructure of base metal **(b)**

Bars cast from this cast iron with the dimensions Φ 25 x 40 mm were subjected to the following volumetric thermal treatments:

- Stresss relief annealing (fig.2.2);
- Softening annealing: (fig.2.3);
- Normalizing (fig.2.4);
- Quenching-tempering (fig.2.5)

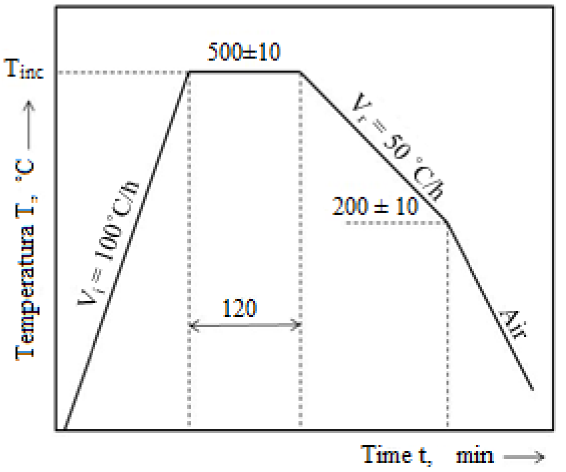

Fig.2.2 Cycle of heat treatment for stress relief annealing

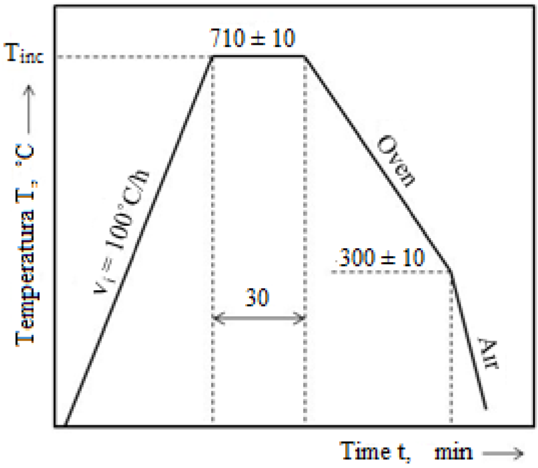

Fig. 2.3 Cycle of heat treatment for softening annealing

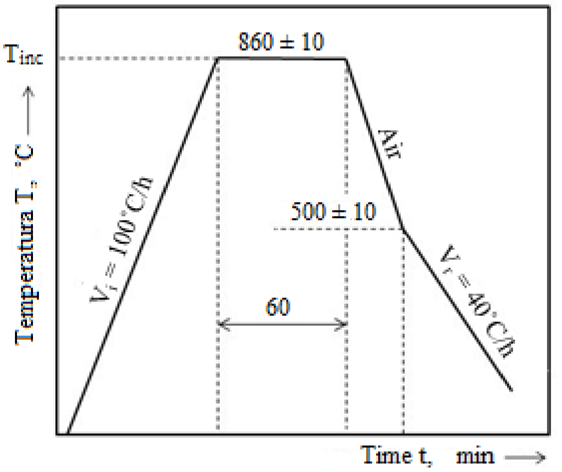

Fig. 2.4 Cycle of thermal treatment for normalization annealing

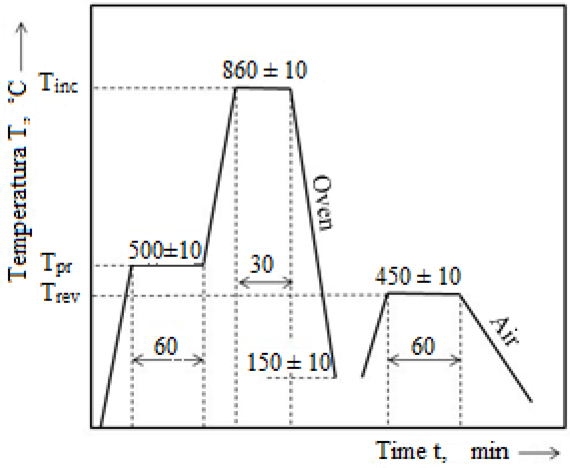

Fig. 2.5 Cycle of thermal treatment for quenching - tempering

Subsequently, samples were taken for cavitation tests (**Fig.2.6)** and for microstructural studies.

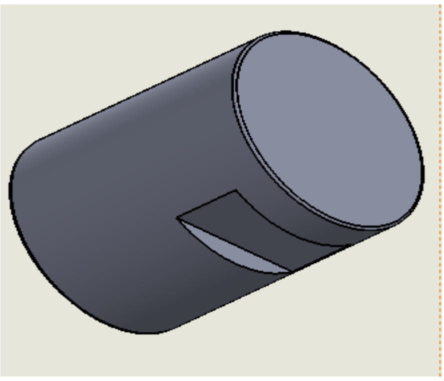

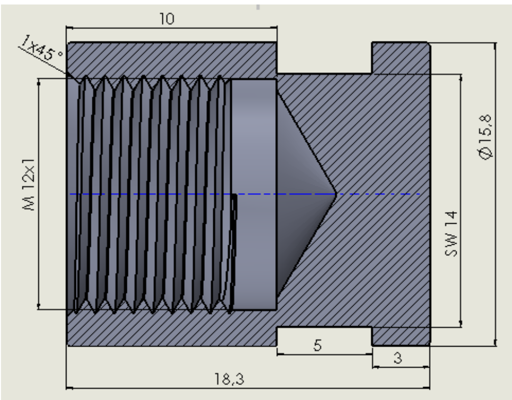

Fig.2.6 Geometry of samples tested at cavitation

The cavitation tests were conducted on a piezoceramic vibrator [20] with piezoceramic crystals **(Fig. 2.7)** made in accordance with the requirements of ASTM G32-2010 [14].

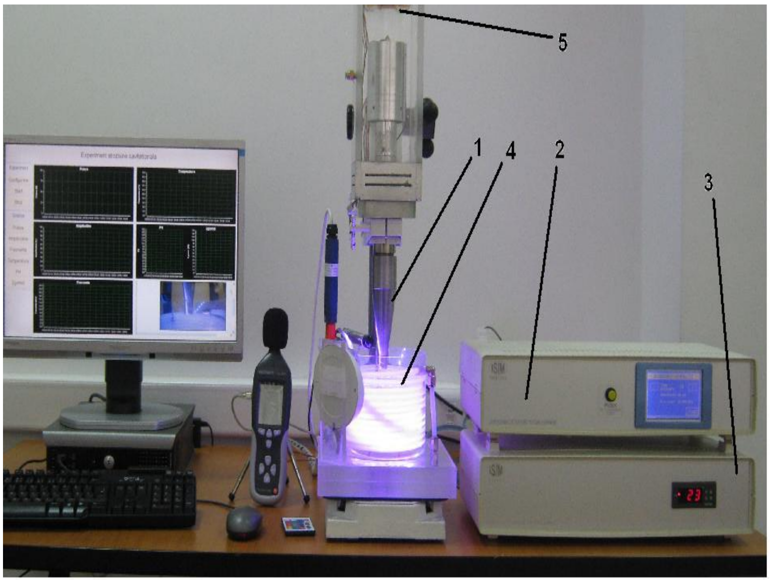

Fig.2.7 Overview (a) and functional scheme (b) of the piezoceramic crystals vibrator: 1-sonotrode; 2 - the electronic system; 3 - water temperature controller; 4 - liquid vessel and cooling coil; 5 - ventilation system

On the basis of the researches carried out, it was possible to compare comparatively the effect of the volumetric thermal treatments taken into account on the cavitation erosion behavior of this class of cast iron. In **Fig. 2.32** are presented the cavitational erosion curves for the four thermal treatment variants applied, noting the differences in behavior of the same material depending on the microstructure obtained. The most favorable values for MDEs and MDERs offer heat treatment - rebound, and most unfavorable, annealing treatment for softening. Sufficiently good values are obtained after annealing for normalization, which can be applied either as a preliminary heat treatment or as a final heat treatment.

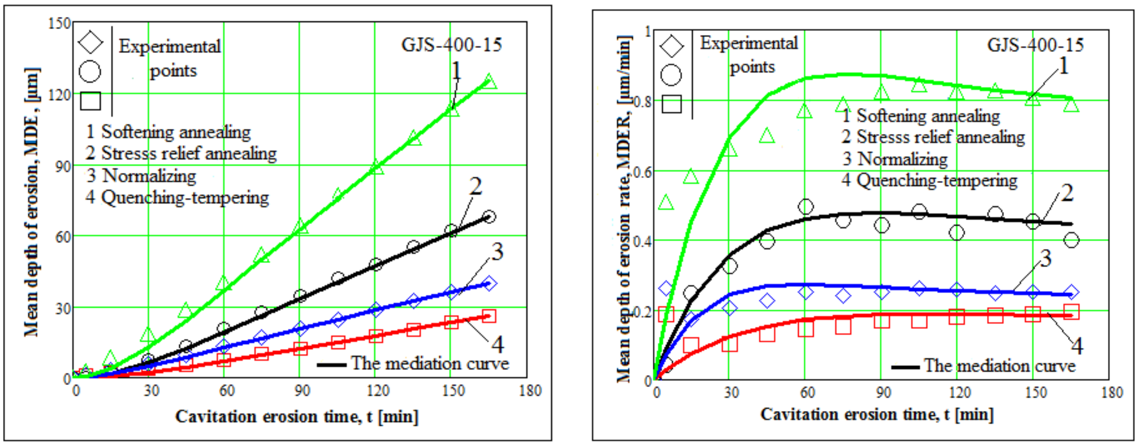

-a- -a-

Fig. 2.32 Cavitation erosion curves for the four variants of thermal treatment: **a** - mean depth of erosion penetration; **b** - erosion speed

2.6 Roughness measurements

The comparative analysis of the degree of surface damage following cavitation tests proves once again the beneficial effect of the final thermal treatment applied to the cavitation behavior of the studied iron, even if the removal of graphite, which is a non-metallic inclusion, the respective portions of the material surface become more rough. From **fig. 2.35 a ... d** it can be seen that the basic metal mass keeps more favorable values if it has undergone the quenching-tempering heat treatment.

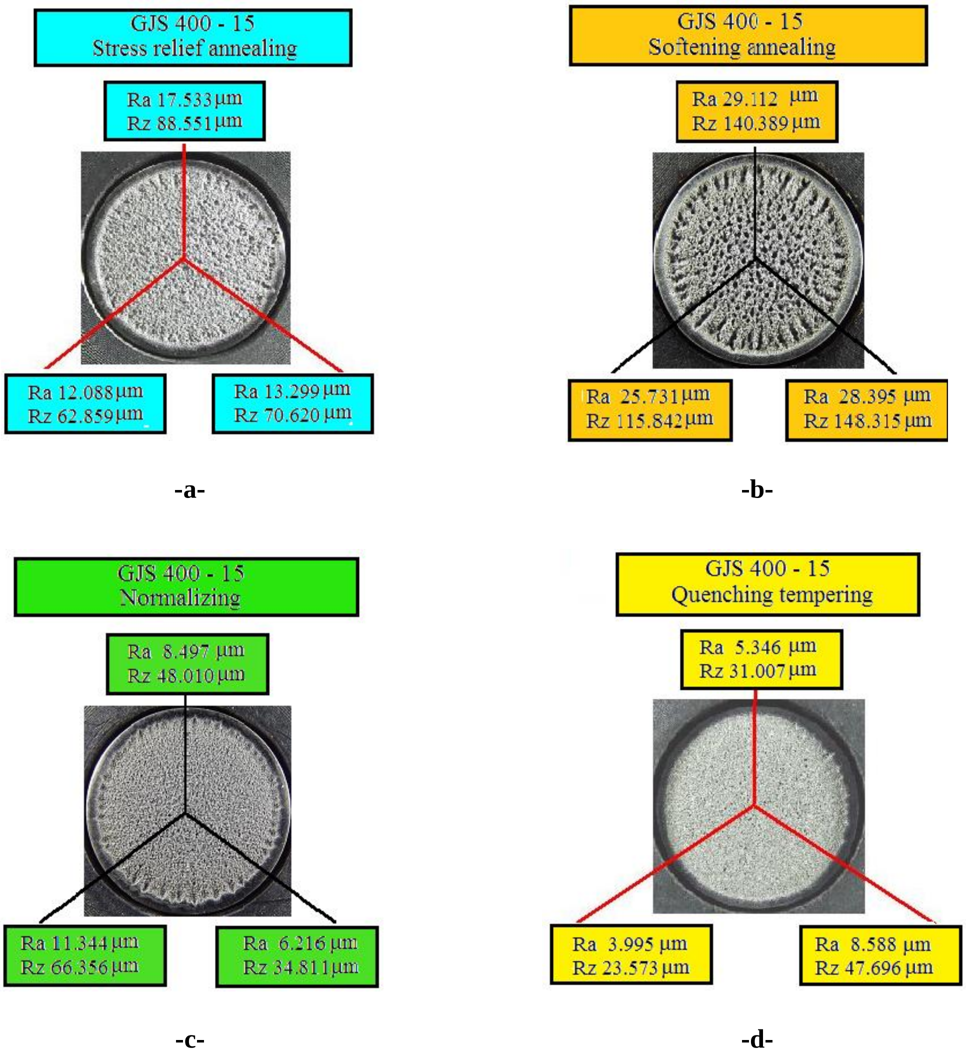

Fig.2.35 The roughness values of Ra, Rz in three directions of measurement for the four structural states: a - swtresss relief annealing; b –softening annealing; c - normalization; d - quenching + tempering

2.7 Hardness tests

The results obtained are centralized in **Table 2.3**, and on the basis of the average values the histogram shown in **Fig. 2.42**. The data presented demonstrate that there is a full concordance between the hardness and the opposite material resistance to degradation by cavitation erosion. The lowest hardness values are specific to the annealing heat treatment (about 178 HV5) and correspond to the highest erosion rate (0.804 µm / min.) And the worst roughness (Rz = 134.848 µm). Instead, the heat-curing heat treatment provides a high hardness (about 462 HV5) which favors a decrease of the erosion rate (0.182 µm / min.) And implicit minimum roughness values (Rz = 34.092 µm).

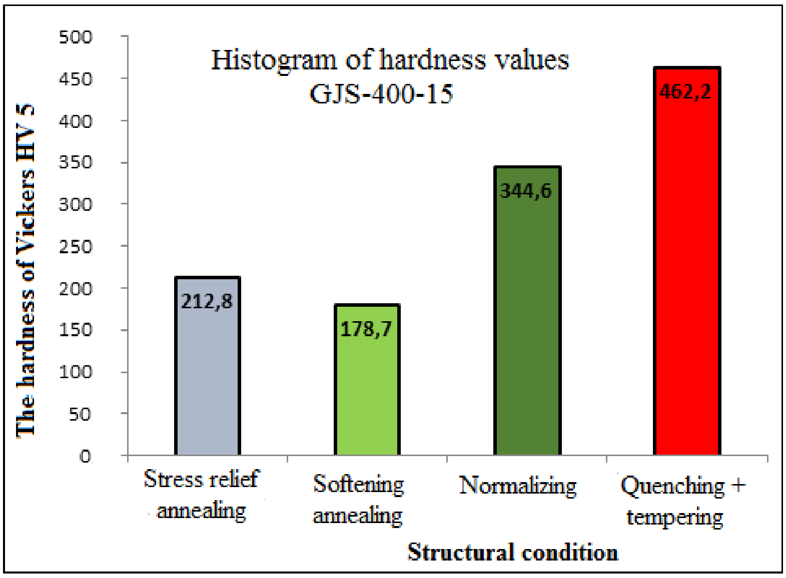

Fig. 2.42. Histogram of hardness values, GJS-400-15

The relationship between the hardness of the applied thermal treatments, the **Rz** roughness of the cavitatively tested surfaces for 165 minutes. and the sizes that characterize cavitation behavior (MDERs, Rcav.) is shown in **FIG. 2.43**. The higher the hardness, the lesser the roughness of the cavitatively attacked surface, and the cavitation behavior is better.

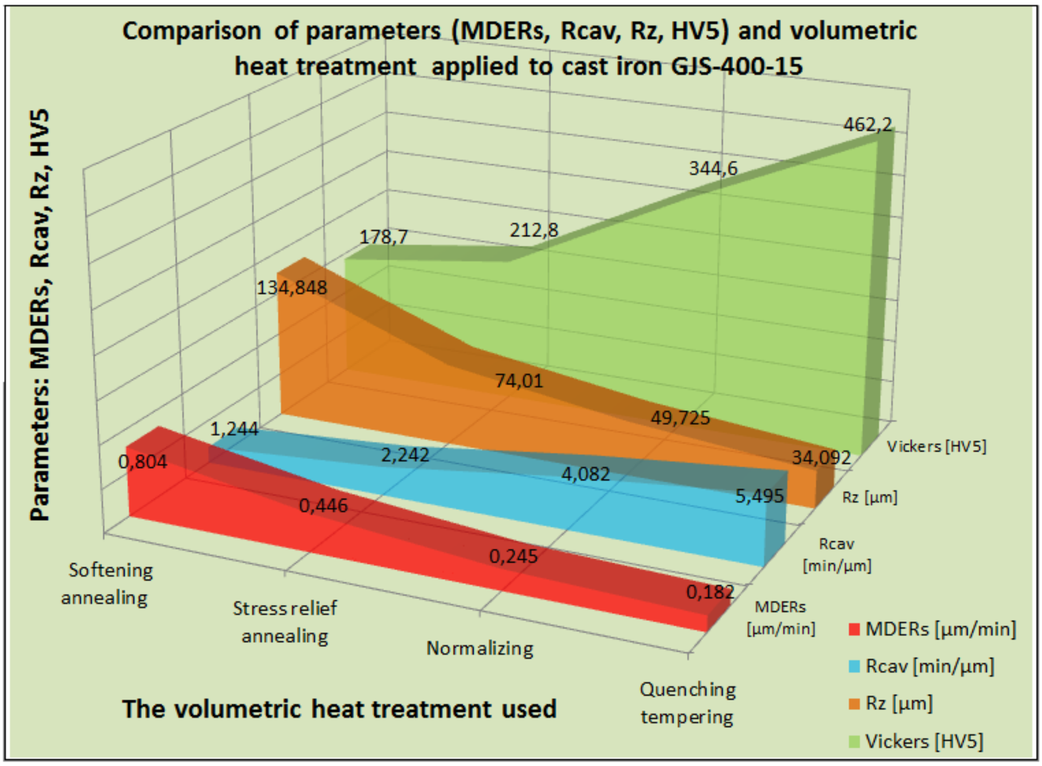

Fig.2.43 Correlation between hardness, roughness and cavitation parameters of nodular cast iron GJS-400-15

Chapters 3

IMPROVING RESISTANCE TO CAVITATION EROSION BY WIPING THE TIG SURFACE

3.2 Concept of surface melting device

This device was designed and built to be able to perform and test the local surface resistivity of samples by the WIG process.
The main components of the device are shown in **Fig. 3.6**:

1. Metal support
2. Positioning device
3. The displacement device (horizontal-vertical)
4. Pendulum device
5. Power supply of the feed device (horizontal-vertical)
6. Pulley feed supply
7. The limit switches
8. TIG welding gun
9. welding source INVERTIG PRO DIGITAL 350 AC / DC

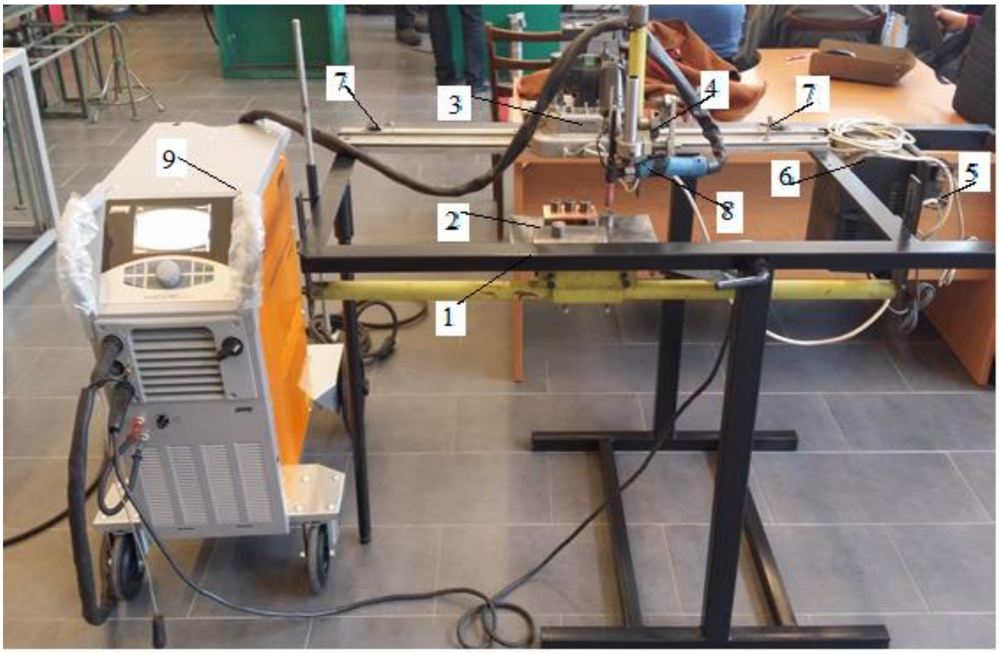

Fig.3.6 Overview of the device used

Surface refinement experiments were conducted for four current values: 60 A, 70 A, 80 A and 90 A. The macroscopic appearance of locally retured samples for the four current values is shown in **Fig. 3.9**. The parameter sets as well as all relevant information, including error messages, are displayed on the computer screen. In the upper middle, the current value of the parameter being accessed is displayed. **Figure 3.12** illustrates the display of the technological parameters for the selected values of the current, respectively for the 4 values of the linear energy.

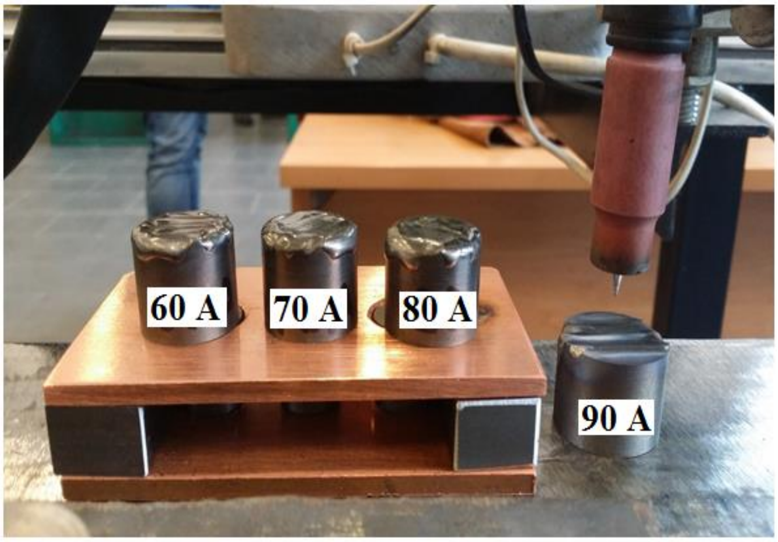

Fig.3.9 The image of locally retouched samples at different currents

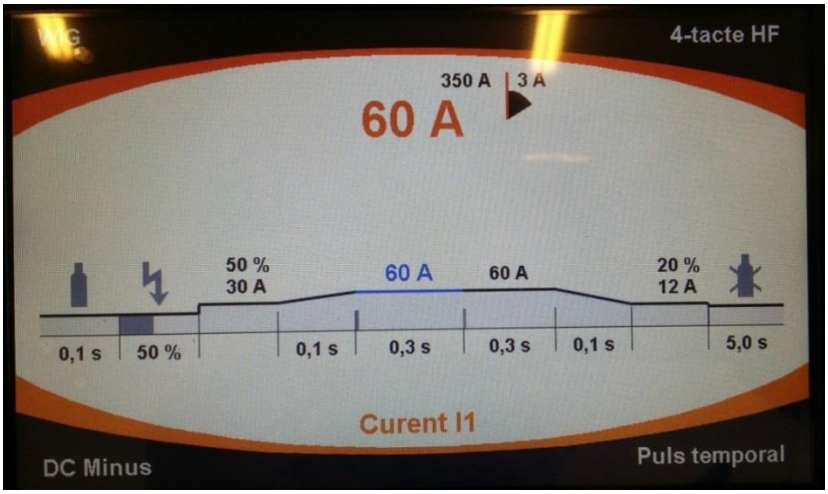

Current (I)	I = 60 A
Arc tension (Ua)	Ua = 9,5 V
Travel speed (V)	V = 10 cm / min
The distance between the electrode and the piece (L)	L = 1,5 mm
Step between rows (P)	P = 3 mm
Linear Energy (El)	$El = \frac{Ua \times I}{V} \times 60 = 3420\ [j/cm]$

Fig.3.12 Cycle of 60 A current and operating parameters

Subsequently, samples were taken for hardness tests, cavitation tests, microstructural studies, X-ray diffraction and cavity surface roughness measurements.

3.3.2 Specific curves and characteristic parameters of cavitation erosion

Cavitation tests were performed in accordance with the methodology presented in Chapter 2 of the paper. For each structural state of the material, three samples were tested, the surface of which was polished to a roughness Ra = 0,051 ÷ 0,090 μm.

Based on the **Δmi** mass losses recorded at the end of each intermediate test period, **"i",** the cumulative mass losses m were determined, and the experimental values for the mean erosion penetration depths of the MDE and its velocity were determined The use of approximation curves is important because, depending on their shape and the dispersion of experimental points against them, it is possible to assess the behavior and resistance to cavitation during the attack.

In **Fig. 3.18 a, b**, the graphs of time variation of mean depth and erosion penetration velocity characteristic for current I = 60 A are shown.

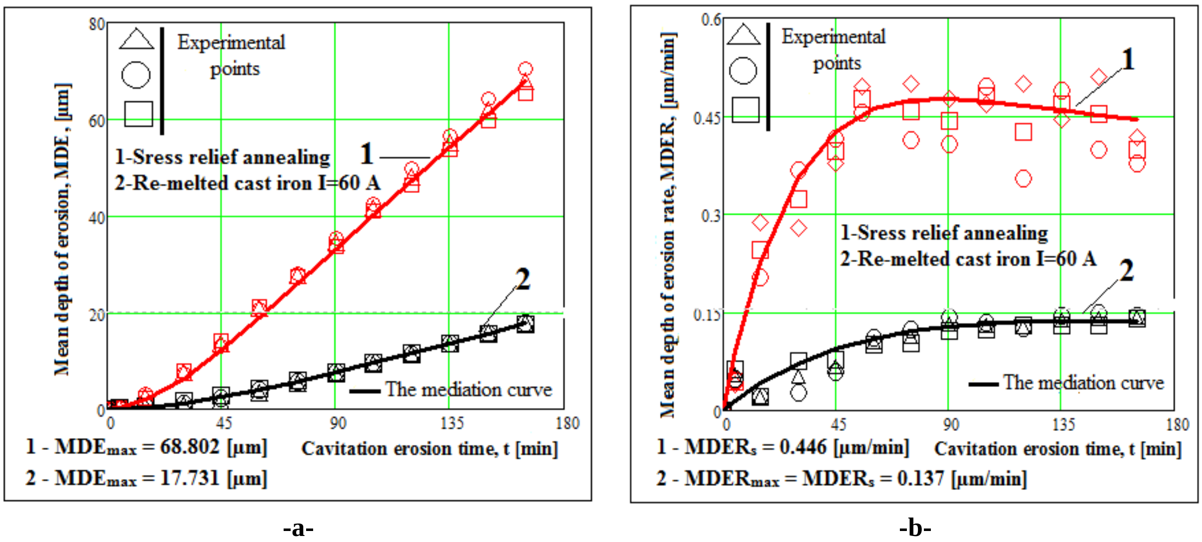

Fig. 3.19 Average erosion penetration depth variation curves (a) and average penetration depth (b) with the duration of cavitation attack for modified TIG surfaces with I = 60 A and for thermal stress relief annealing: 1 - stress annealing; 2 – TIG re- melting, I = 60 A

3.3 Metallographic examinations

Figure 3.21 illustrates the fine microstructure of the marginal layers, consisting of ledeburic eutectic, acicular cementite, dendritic transformed austenite and traces of nodular graphite, undissolved during heating at the melting temperature. The increase in the current from 60 A to 90 A and the linear energy from 3420 J / cm to 5400 J / cm is manifested by a slight increase in the amount of undissolved graphite nodules. Additionally, the 90 A processed higher current layer has a heavier structure with larger dendrites compared to the 60 A less current processing. The explanation is based on the effect of linear energy increase on the reduction the rate of cooling, respectively the degree of under-cooling, the decrease of the number of germs and the increase of the critical radius of germination.

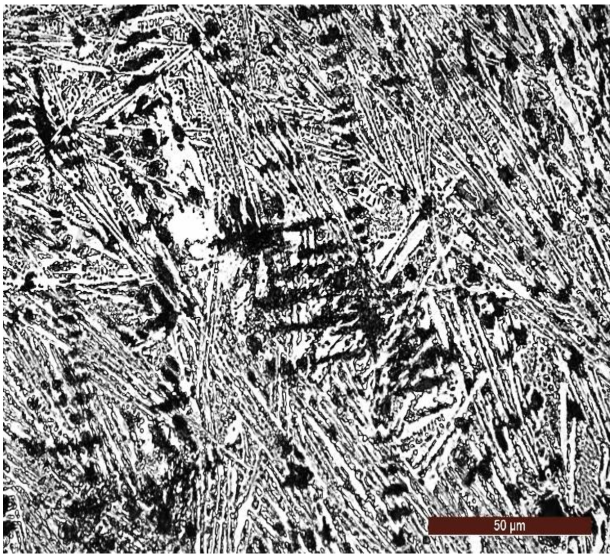

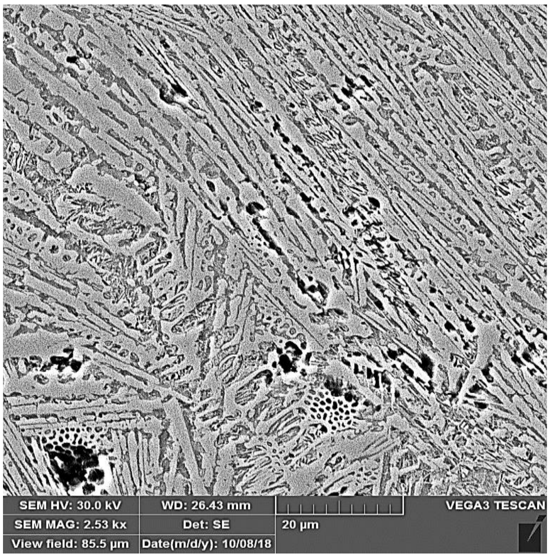

-a- -b-

Fig.3.21 Microstructure of the TIG layer produced by the use of 60 A current: **a -** x200; **b** - x 2500. Chemical attack: 2% NITAL

3.3.5 Microstructure tests on re-melted layers

Gradient gradient curves on the longitudinal section of the TIG re-melted samples on the surface are shown in **Fig.3.29.**

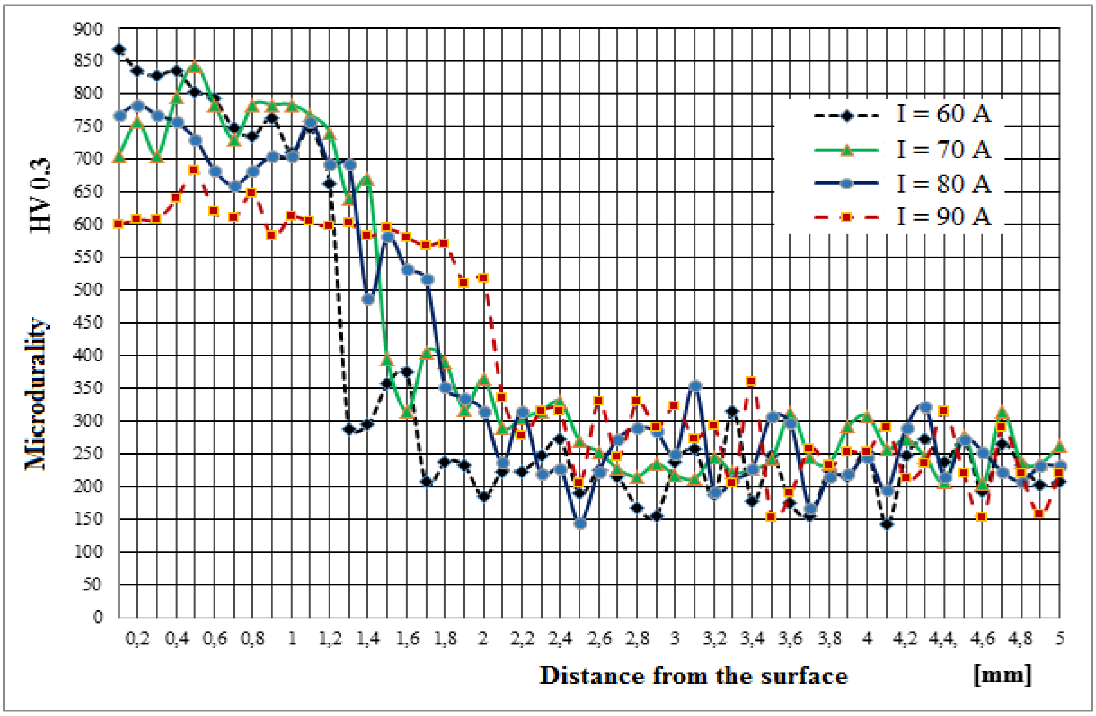

Fig.3.29 The variation of the microstructure on the longitudinal section of the TIG processed samples

They demonstrate that the microdurality of the molten zone has increased significantly compared to the microdurality of the base material. Thus, the area processed at the smallest melting current of 60 A indicates microdurality values ranging from 700 to 850 HV 0.3, while at 90 A it varied between 560 and 680 HV 0.3. The base material has values microdurity, between 200 and 260 HV 0.3. The distribution of hardness on the section of investigated samples shows small fluctuations, which are justified by the microstructural changes generated by the used technique.

Chapters 4

THERMAL SPRAYING WITH THE HIGH SPEED FLAME (HVOF) AND RESISTANCE TO CAVITATION EROSION

4.2 Materials and experimental procedures

For investigations, EN-GJS-400-15 nodular cast iron was used as substrate material and was subjected to stress relief annealing at 500 ± 10 ° C. The atomized gas powder (Amperit 377.065), having the chemical composition similar to AISI 316 L austenitic stainless steel, was used to make layers deposited by the HVOF method. The particle size of the particles was -30 + 10 μm. The thermal spraying process was conducted on a Sulzer Metco equipment **(fig.4.3).**

-a- -b-

Fig.4.3 HVOF spraying equipment: **a** - control module; **b**- DJM 2700 pistol

4.3 Evaluation and interpretation of experimental results

4.3.1 Micrographic analyzes

Figure 4.6 shows laser scanned laser micrographs of longitudinal sections through HVOF coated samples with austenitic stainless steel powders. It is noted that the deposited layer is dense, cracked, with a lamellar structure typical of this coating process. There are no metallic continuity defects on the substrate layer interface.

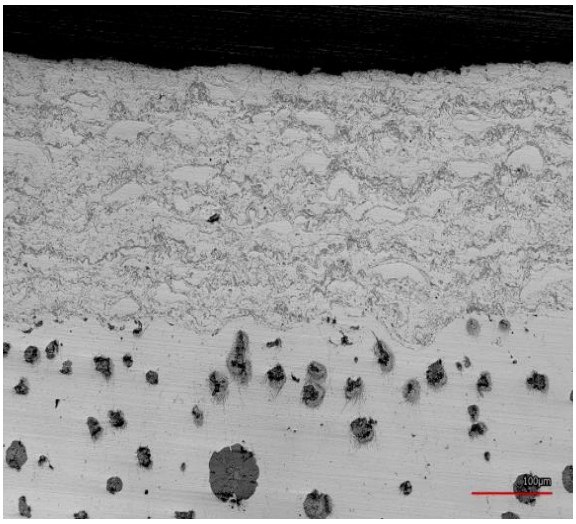

-a- -b-

Fig. 4.6 Laser scanning images: **a** - x 100, layer system - substrate; **b** - x 200, section through the deposited layer

4.3.3 Cavitation curves

The cavitation tests were conducted on two sets of three samples, one being characteristic of the reference material (heat treatment by annealing for strain relief) and the other, the HVOF coating of the austenitic stainless steel powder coating.

In **Figures 4.9** and **4.10** are presented the variation curves of the two parameters that characterize the cavitation resistance according to the duration of the test. It can be noticed that after the coating process, the values of the maximum erosion penetration depth, MDEmax. and erosion rate over the stabilization period, MDERs, are reduced by more than 2 times compared to the reference structural state.

The explanation for this improvement is based on the fine microstructure and the high surface hardness.

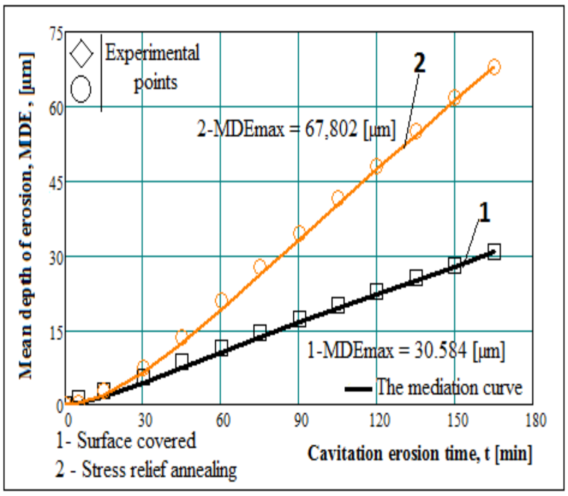

Fig.4.9 Evolution of the average depth of erosion penetration with the duration of cavitation attack: 1 – surface covered ; 2 - surface treated by annealing for strain relief

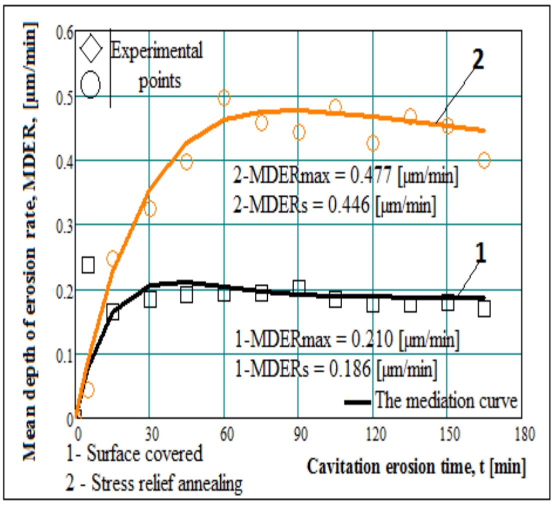

Fig. 4.10 Evolution of average depth of erosion penetration rate with cavitation attack duration: 1 – surface covered; 2 - surface treated by annealing for strain relief

Chapters 5

FINAL CONCLUSIONS AND ORIGINAL CONTRIBUTIONS. NEW RESEARCH DIRECTIONS

The bibliographic studies, the experimental researches and the analyzes carried out within the doctoral program and presented in the thesis lead to the following conclusions and original contributions:

1. Laboratory investigation of cavitation-induced erosion plays an important role in material selection and processing techniques for engine components such as butterfly valves **(Fig. 5.1)** that are exposed to the impact of shock waves and microjet jets produced by cavitation bubble the boundary material defining the flow range.

Valves AVK PN 10 - 16

Double eccentric butterfly valve

Fig.5.1 Butterfly valves

2. The assessment of the behavior and resistance of materials to cavitation erosion is advisable to be made both on the basis of characteristic curves and parameters and on microstructural investigations on degraded surfaces performed at various intermediate and final stages of the cavitation attack.

3. In the cast and de-stressed state, the cavitation erosion rate of the cast iron is approx. 2.62 times higher than C45 steel with a similar hardness, phenomenon which is explained by the effect of concentration of the stresses created by the expelled graphite from the base metal mass.

4. As compared to annealing for strain relief, the thermal normalization treatment provides a cavitation resistance increase of about 3.16 times the maximum value of the cumulative average depth of erosion (MDE (t) curve) and about 3.28 times according to the values to which the speed parameter is stabilized, MDER.

5. The quenching-tempering heat treatment the applied to ferrite-perllite nodular cast iron determines a reduction of the average erosion depth of approx. 2.60 times and the speed of approx. 2.45 times, compared to the structural state obtained by heat treatment by annealing for strain relief.

6. Scanning by optical microscopy and scanning electron microscopy of degraded surfaces and longitudinal sections through the cavity samples highlights that the initiation of the cavities (at all volume treatment regimes applied) takes place on the interface between ferrite and nodular graphite and is determined by a microglobal activity and mechanical factors. With the increase of the cavitational attack time, partial fragmentation and expulsion of the graphite nodules occur.

7. The increase in the proportion of perlite in the microstructure following the application of the normalization treatment as well as the return martensite structure obtained in the quenching-tempering heat treatments justifies the improvement of cavitation resistance since both structural constituents having higher mechanical strength characteristics will resist deformation surface.

8. The method of local melting of the surface of the nodular casting using as a source of heat the TIG electric arc, operated at 60 ... 90 A and 9.5-10 V, has led to a significant improvement in cavitation erosion resistance. Compared to the structural state obtained from the annealing thermal treatment for stress relief, the layers processed at the 60 A current show a decrease in erosion penetration velocity times, respectively an increase in cavitation erosion resistance times. For higher processing currents of 90 A, the erosion penetration rate is reduced by 1.93 times, and cavitation resistance increases by approx. 1.93 or.

9. The rapid heating of the surface of the parts causes complete or partial dissolution of the graphite nodules, and the primary and secondary crystallization of the molten metal bath is produced by the Fe-Fe3C metastable system so that a fine structure is formed in the marginal layer of white cast iron (Ledeburita + Transformed Austenite), and underneath it a hardened layer (Martensite + Cement + Nodular Graphite).

10. SEM images concerning TIG melted and cavity-eroded surfaces have highlighted the formation of small craters with depths below 1 mm. which did not penetrate into the substrate; The removal of the material is attributed to the initiation of fatigue cracks on the interface of the superimposed regions of the layer.

11. The surface of the AISI 316 L austenitic stainless steel powder coated parts, operating in cavitation mode, leads to an average depth of erosion after 165 minutes of cavitation attack, reduced by approx. 2,21 or compared to the structural state obtained by annealing for strain relief and an erosion penetration rate of approx. 2.39 or less.

New research directions

Based on the research carried out within this doctoral program, the results obtained and presented in the paper, the following perspectives can be formulated for future research:

1. Widening the database of new surface coating methods and thermal and thermo-chemical treatment technologies that can be applied to nodular cast iron parts in order to increase cavitation erosion resistance.
2. Investigation of the structural degradation of these types of cast iron during the incipient cavitation period.

Bibliografie:

[1] A. Amirsadeghi, M.S. Heydarzadeh, S.F. Kashani Bozorg. *Effects of TIG surface melting and chromium surface alloying on microstructure, hardness and wear resistance of ADI.* J. Iron Steel Res. Int., 15 (2008), pp. 86-94

[2] A. Amirsadeghi, M.S. Heydarzadeh. *Comparison of the influence of molybdenum and chromium TIG surface alloying on the microstructure, hardness and wear resistance of ADI.* J Mater Process Technol, 201 (2008), pp. 673-677

[3] A. Gulzar, J.I. Akhter, M. Ahmad, G. Ali, M. Mahmood, M. Ajmal.*Microstructure evolution during surface alloying of ductile iron and austempered ductile iron by electron beam melting.* Appl Surf Sci, 255 (2009), pp. 8527-8532

[4] A. Roy, I. Manna: *Laser surface engineering to improve wear resistance of austempered ductile iron.* Mater Sci Eng A, 279 (2001), pp. 85-93

[5] Abouel-Kasem, A.; Ezz El-Deen, A.; Emara, K.M. and Ahmed S.M., 2009, "*Investigation Into Cavitation Erosion Pits"* Journal of Tribology, 131, 31605-031612..

[6] Alabeedi KF, Abboud JH, Benyounis KY. *Microstructure and erosion resistance enhancement of nodular cast iron by laser melting*. Wear 2009, 266, pp. 925–933

[7] Amirsadeghi A, Heydarzadeh MS, Kashani Bozorg SF. *Effects of TIG surface melting and chromium surface alloying on microstructure, hardness and wear resistance of ADI.* J. Iron Steel Res. Int. 2008,15, pp. 86–94

[8] Amirsadeghi A, Heydarzadeh MS. *Comparison of the influence of molybdenum and chromium TIG surface alloying on the microstructure, hardness and wear resistance of ADI.* J. Mater. Process. Technol. 2008,201, pp. 673–677

[9] Annual Book of ASTM Standards (2010) Section 3: *metals test methods and analytical procedures*, vol 03.02. Annual Book of ASTM Standards, West Conshohocken

[10] Anton, I.. : *Cavitaţia, Vol I*, Editura Academiei RSR, Bucureşti, 1984

[11] Anton, I.. : *Cavitaţia, Vol II*, Editura Academiei RSR, Bucureşti, 1985

[12] Balan K. P., a.o.: *The influence of microstructure on the erosion behaviour of cast irons*. Wear, Vol. 145, Issue 2, 1991, pp. 283 – 296

[13] **Bena T**. Mitelea I.,Bordeasu I., Crăciunescu C. *The effect of the softening annealing and of normalizing on the cavitation erosion rezistance of nodular cast iron fgn 400-15.* Metal 2016 International Conference on Metalurgy and Materials, pp. 653-658, ISBN 978-80-87294-67-3 (ISI Proceedings)

[14] **Bena T**. Mitelea I.,Bordeasu I., Utu D., Crăciunescu C. *The quenching – tempering heat treatament and cavitation erosion resistance of nodular cast iron with ferrite – pearlite microstructure.* Metal 2017 International Conference on Metalurgy and Materials, pp.118, ISBN 978-80-87294-73-4 (ISI Proceedings)

[15] Benyounis KY, Fakron OM, Abboud JH. *Rapid solidification of M2 high-speed steel by laser melting*. Mater. Des. 2009, 30, pp. 674–678

[16] Benyounis KY, Fakron OMA, Abboud JH, Olabi AG, Hashmi MJS. *Surface melting of nodular cast iron by Nd-YAG laser and TIG. J. Mater*. Process. Technol. 2005,170, pp. 127–132

[17] Berchiche, N. A.; Franc, J. - P. and Michel, J. M., 2002, "*A cavitation erosion model for ductile materials.* Journal of Fluids Engineering, 124(3), 601–606.

[18] Bo Sun, Hirotaka Fukanuma, Naoyuki Ohno, *Study on stainless steel 316L coatings sprayed by a novel high pressure HVOF,* Surface & Coatings Technology. 239(2014) 58-64, http://dx.doi.org/10.1016/j.surfcoat.2013.11.018

[19] Bordeaşu I. : *Eroziunea cavitaţională a materialelor.* Editura Politehnica Timişoara, 2006
[20] Bordeaşu I., Mitelea I.: *Cavitation erosion behavior of stainless steels with constant Nichel and variable Chromium content*, Materials Testing, Volume 54, Issue 1, pp. 53-58, 2012.
[21] Bordeasu I**.,** Patrascoiu C., Badarau R., Sucitu L., Popoviciu M., Balasoiu V., *New contributions in Caviation Erosion Curves Modeling,* FME Transactions Fakulty of Mechanical Engineering, vol.34 Nr.1/2006, University of Belgrade, 2006, YU ISSN 1451-2092, p.39-44
[22] Bordeasu I., Popoviciu M., Mitelea I., Ghiban B., Balasoiu V., Tucu D., *Chemical and mechanical aspects of the cavitation phenomena,* Chem.Abs. RCBUAU 58(12) Revista de chimie Vol.58 Nr.12, 2007, pp 1300-1304
[23] Burca M., **Bena T.A**., Lucaciu I., Husi G. *Aspects of root protection in welding. Nonconventional Technologies Review* – no.2/2011Vol.XV, pp.25-30, ISSN 1454-3087
[24] Burca M., Lucaciu I., **Bena T.A**. *Device for swinging the welding torch during ascending vertical MIG/MAG welding.* Annals of the Oradea University Fascile of managment and Technological Engineering, 2012 Volume XI (XXI),2012.Nr.1, pag.4.24-4.34, ISSN 1583-0691
[25] C.H. Chen, C.P. Ju, J.M. Rigsbee: *Laser surface modification of ductile cast iron***.** Mater. Sci. Technol., 4 (1988), p. 161
[26] Chahine, G. L., Franc, J.-P. and Karimi, A., *"Laboratory Testing Methods of Cavitation Erosion"*, in Kim, K.-H. et al. (eds.), Advanced Experimental and Numerical Techniques for Cavitation Erosion Prediction, Fluid Mechanics and Its Applications 106, Springer Science+Business Media Dordrecht 2014.
[27] Choi, J.-K., Jayaprakash, A. and Chahine, G. L., 2012, "*Scaling of Cavitation Erosion Progression with Cavitation Intensity and Cavitation*", Wear, 278–279, 53–61.
[28] Dai WS, Chen LH, Lui TS. SiO_2 particle erosion of spheroidal graphite cast iron after surface remelting by the plasma transferred arc process. Wear 2001, 248, pp. 201–210
[29] Designation: G 32-09: *Standard Test Method for Cavitation Erosion Using Vibratory Apparatus.* Annual Book of ASTM Standards (2010) Section 3: Metals test methods and analytical procedures, vol 03.02. West Conshohocken, pp 94–109
[30] Dojcinovic M.; Olivera E.: *The morphology of ductile cast iron surface damaged by cavitation, Metall.* Mater. Eng. Vol 18 (3) 2012 p. 165-17.
[31] E.Sadeghimeresht, N.Markocsan, P.Nylén, *Microstructural characteristics and corrosion behavior of HVAF- and HVOF-sprayed Fe-based coatings*, Surface and Coatings Technology Volume 318, 25 May 2017, Pages 365-373
[32] Espitia A.L., Toro A.: *Cavitation resistance, microstructure and surface topography of materials used for hydraulic components.* Tribology International, Vol. 43, 2010, pp. 2037 – 2045
[33] Franc J.P., Michel J.M., ş.a., La Cavitation, *Mecanismes phisiques et aspects industriels*, Press Universitaires de GRENOBLE, 1995
[34] Franc, J.-P., 2009, *"Incubation Time and Cavitation Erosion Rate of Work-Hardening Materials"*, Journal of Fluids Engineering, 131(2), 021303-021317.
[35] Frank J.P., Michel J.M., *Fundamentals of cavitation.* Kluwer Academic Publishers-Dordrecht/Boston/London. 2004
[36] G.L. Hou, X.Q. Zhao, H.D. Zhou, J.J. Lu, Y.L. An, J.M. Chen, J. Yang, *Cavitation erosion of several oxy-fuel sprayed coatings tested in deionized water and artificial seawater,* Wear 311 (2014) 81–92
[37] Gadag S.P. , Srinivasan M.N. : *Cavitation erosion of laser-melted ductile iron.* Journal of Materials Processing Technology, Vol. 51, Issues 1-4, 1995, pp. 150 – 163

[38] Garcia R., Hammitt F. G., Nystrom R.E., *Corelation of cavitation damage with other material and fluid properties,* Erosion by Cavitation or Impingement, ASTM, STP 408 Atlantic City, 1960

[39] Georgevici I. : *Contribuţii privind dezvoltarea unor oţeluri inoxidabile cu transformare martensitică directă,* Teză de doctorat, Timişoara, 2003

[40] Geru N. şi alţii : *Materiale metalice – structură, proprietăţi, utilizări.* Editura tehnică Bucureşti, 1985

[41] Gulzar A, Akhter JI, Ahmad M, Ali G, Mahmood M, Ajmal M. *Microstructure evolution during surface alloying of ductile iron and austempered ductile iron by electron beam melting.* Appl. Surf. Sci. 2009, 255, pp. 8527–8532

[42] Hashem – Al A., a.o.: *Cavitation corrosion of nodular cast iron (NCl) in seawater* : Microstructural effects. Materials Characterization, Vol. 47, Issue 5, 2001, pp. 383 – 388

[43] Hattori S.; Kitagawa T.: *Analysis of cavitation erosion resistance of cast iron and nonferrous metals based on database and comparison with carbon steel data*, Wear, Volume 269, Issue 5-6, 2010, pp. 443-448.

[44] Heydarzadeh M.S. , Karshenas G. , Boutorabi S.M. : *Electron beam surface melting of as cast and austempered ductile irons.* J Mater Process Technol, 153–154 (2004), pp. 199-202

[45] Heydarzadeh MS, Karshenas G, Boutorabi SM. *Electron beam surface melting of as cast and austempered ductile irons.* J. Mater. Process. Technol. 2004, 153– 154, pp. 199–202

[46] Hiraoka T, Nakamora Y, Tanaka Y. *Mechanical properties of cast iron surface hardened by TIG arc remelting.* Trans. Am. Foundrymen’s Soc. 1995(102, 603

[47] Hug E., a.o.: *Application of the Monkman – Grant law to the creep fracture of nodular cast irons with various matrix compositions and structures*. Mat. Science and Engineering : A, Vol. 518, Issues 1 – 2, 2009, pp. 65 – 75

[48] I.D. Uţu, I. Mitelea: *Introducere în ingineria materialelor*. Editura Politehnica, Timişoara, 2018, pp.167-181

[49] IMitelea, **T. Bena**, I. Bordeasu, C.M. Craciunescu, *Relationships Between Microstructure, Roughness Parameters and Ultrasonic Cavitation Erosion Behaviour of Nodular Cast Iron, EN-GJS-400-15*, REV.CHIM.(Bucharest) 69 No. 3 2018

[50] Ishida T. *Local melting of nodular cast iron by plasma arc*. J. Mater. Sci. 1983,18, pp.1773–1784

[51] Jean M, Tzeng Y. *Optimization of electron-beam surface hardening of cast iron for high wear resistance using the Taguchi method*. Int. J. Adv. Manuf. Technol. 2004, 24, pp.190–198

[52] Jing Yua, Bo Song, Yanchuan Liu, *Microstructure and wear behaviour of Ni-based alloy coated onto grey cast iron using a multi-step induction cladding process*, Results in Physics 10 (2018) 339–345, DOI: 10.1016/j.rinp.2018.06.042

[53] K.F. Alabeedi, J.H. Abboud, K.Y. Benyounis: *Microstructure and erosion resistance enhancement of nodular cast iron by laser melting.* Wear, 266 (2009), pp. 925-933

[54] K.Y. Benyounis, O.M. Fakron, J.H. Abboud: *Rapid solidification of M2 high-speed steel by laser melting.* Mater. Des., 30 (2009), pp. 674-678

[55] K.Y. Benyounis, O.M.A. Fakron, J.H. Abboud, A.G. Olabi, M.J.S.Hashmi: *Surface melting of nodular cast iron by Nd-YAG laser and TIG.* J Mater Process Technol, 170 (2005), pp. 127-132

[56] Kowk C.T., Cheng F.T., Man H.C. : *Laser surface modification on UNS S31603 stainless steel using NiCrSiB alloy for enhancing cavitation erosion resistance*, Surface and Coatings Technology, vol. 107, Issue 1, pp. 31-40, 1998

[57] Kurylo P.: *Possibility of plastic processing of spheroidal cast iron*. Procedia Engineering, Vol. 48, 2012, pp. 326 – 331

[58] L.C. Chang, I.C. Hsui, L.H. Chen, T.S. Lui: *Influence of graphite nodules on the particles erosion of spheroidal graphite cast iron.* Wear, 257 (2004), pp. 1125-113

[59] M. Shamanian, S.M.R. Mousavi Abarghouie, S.R. Mousavi Pour: *Effects of surface alloying on microstructure and wear behavior of ductile iron.* Mater. Des., 31 (2010), pp. 2760-2766

[60] Matsumura I., Okumoto S., Saga Y : Effects of tensile stress on cavitation erosion, Werkstoffe und Korrosion, vol.30, pp.462-498, 1979

[61] Mitelea I., Bordeaşu I., Hadăr A. : *Cavitation erosion characteristics of stainless steel with controlled transformation,* Revista de chimie Bucureşti, Chem. Abs. RCBUAU 57 (2) (117-228), vol. 57, nr. 2, pp.215-220, febr. 2006

[62] Mitelea I., Tillmann W. – Ştiinţa materialelor vol. II, ed. Politehnica, Timişoara, 2007

[63] Mitelea I., Tillmann W. : *Ştiinţa materialelor, Vol. I,* Editura Politehnica Timişoara, 2006

[64] Mitelea, I., Bordeasu, I., Pelle, M., Craciunescu, C. M., *Ultrasonic cavitation erosion of nodular cast iron with ferrite-pearlite microstructure,* ULTRASONICS SONOCHEMISTRY, Volume: 23, MAR 2015, Pages: 385-390

[65] Okada T, Iwai Y, Yamamoto A. *A study of cavitation erosion of cast iron*. Wear 1983, 84, pp. 297–312, DOI: 10.1016/0043-1648(83)90271-5

[66] Pai R. and Hargreaves, D.J., 2002, "*Performance of environment-friendly hydraulic fluids and material wear in cavitating conditions",* Wear, 252, 970–978.

[67] Popoviciu O.M., Bordeaşu I., *Tehnologia fabricaţiei sistemelor hidraulice,* Editura Politehnica, Timişoara, 1998

[68] R. Arabi Jeshvaghani, M. Shamanian, M. Jaberzadeh: *Enhancement of wear resistance of ductile iron surface alloyed by stellite 6.* Mater Des, 32 (2011), pp. 2028-2033

[69] Riemschneider E., Bordeaşu I., Micu L.M., Pîrvulescu L.D., **Bena T.,** Bădărău R. *Studiul eroziunii oțelului Ust 37-2 prin cavitație vibratoare*. Revista Știința și Inginerie Vol.32, pp. 327-332

[70] Ripoşan I., Sofroni L. : *Fonta bainitică*. Editura tehnică Bucureşti, 1989

[71] Roy A, Manna I. Laser surface engineering to improve wear resistance of austempered ductile iron. Mater. Sci. Eng. A 2001,279, pp. 85–93

[72] Singh, R.; Tiwari, S. K. and Mishra Cavitation S. K., 2012 *"Erosion in Hydraulic Turbine Components and Mitigation by Coatings: Current Status and Future Needs"*, Journal of Materials Engineering and Performance, 21(7) 1539-1551.

[73] Sofroni L : *Elaborarea şi turnarea aliajelor*. Editura Didactică şi Pedagogică Bucureşti, 1985

[74] *** Standard test method for cavitation erosion using vibratory apparatus ASTM G32-2010

[75] T. Ishida: *Local melting of nodular cast iron by plasma arc*. J. Mater. Sci., 18 (1983), pp. 1773-1784

[76] Thiruvengadam A., Preiser H. S., - *On testing materials for cavitation damage resistence,* Report. 233 – 3, 1963

[77] Tomlinson W.J. , Megaw J.H.P.C. , Bransden A.S. , Girardi M. : *The effect of laser surface melting on the cavitation wear of grey cast iron in distilled and 3% salt waters*. Wear, Volume 116, Issue 2, 1 May 1987, pp. 249-260

[78] W.S. Dai, L.H. Chen, T.S. Lui: *SiO_2 particle erosion of spheroidal graphite cast iron after surface remelting by the plasma transferred arc process*. Wear, 248 (2001), pp. 201-210